Influence of matrix-filler thermal conductivity on micro heat transfer in two-component composites

To cite this article: A Pysarenko and I Zaginaylo 2021 *IOP Conf. Ser.: Mater. Sci. Eng.* **1162** 012013

View the article online for updates and enhancements.

Influence of matrix-filler thermal conductivity on micro heat transfer in two-component composites

A Pysarenko[1] and I Zaginaylo[1]

[1] Department of Physics, Institute of Civil Engineering, Odessa State Academy of Civil Engineering and Architecture, Didrikhsona st., 4, Odessa, 65029, Ukraine

E-mail: pysarenkoan@gmail.com

Abstract. The maps of local heat fluxes in the composite matrix with randomly located heat-insulating and heat-conducting inclusions have been calculated in this work. It was shown that with a significant difference in the thermal conductivity of inclusions and matrix, the main heat transfer occurs through the induced heat-conducting channels. It was found that the weighted average angles of local heat fluxes deviation from the direction of the temperature difference between the sample faces depend on the concentration of heat-insulating and heat-conducting inclusions of various sizes. A sublinear decrease or super linear increase in the effective thermal conductivity of the composite with an increase in the concentration of heat-insulating or heat-conducting inclusions, respectively, was associated with a change in the path length of local heat fluxes due to the flow at an angle to the direction of the temperature difference. An approximation formula for the dependence of the composite effective thermal conductivity on the filler concentration has been proposed, which makes it possible to take into account the presence of both heat-conducting and heat-insulating inclusions.

1. Introduction

The development of new, high-quality and cost-effective materials determines the development path of modern industry. The quantitative characteristics of new materials, as a rule, vary in wider ranges and, thus, correspond to the requirements for the operation of the finished product.

The possibility of changing the properties of composite materials, in particular the quantitative and qualitative characteristics of the filler, the physicochemical characteristics of the matrix, determines their competitiveness in relation to traditional materials. However, the economic efficiency of new materials largely depends on the ability to predict their basic integral and local characteristics, as well as operational properties. Great efforts are being made to improve the properties of composite materials and especially thermal conductivity. A wide range of changes in the thermal conductivity of a composite material determines a wide range of applications for these materials.

The concept of effective thermal conductivity makes it possible to determine in detail the behavior of composites from a technological point of view, which is an undoubted advantage of using composites in technological chains.

Now, there are a large number of theoretical and empirical models for predicting effective thermal conductivity [1 - 3]. However, despite the theoretical and technological importance of this property and a significant amount of research carried out, both the functional behavior and quantitative estimates of the value of composite effective thermal conductivity have not been sufficiently studied.

The reason for these difficulties is that the effective thermal conductivity is a complex function of the thermal conductivity of the filler and matrix [4], the geometry and spatial distribution of inclusions, filler-matrix thermal contact resistance [5]. The scope of analytical methods for solving problems of heat conduction comprises a fairly limited number of types of applications in which the geometry object is presented only simple shapes (circle, rectangle, fiber and so on).

An additional factor that complicates the theoretical description of heat transfer in composites is the random spatial distribution of the filler particles [6], as well as its multifractionality [7].

Spatial graded composites have a wide range of uses. The matrix of such composites includes two or more components. The relative volume fractions of the components or the sizes of the filler particles change in the volume of the matrix according to a fixed law [8].

Thermal anisotropy of composites with spatial gradation leads to the appearance of effective thermal barriers and nonlinear heat fluxes.

The numerical experiment method is practically the only method for predicting the thermophysical properties of both composite materials with a randomly inhomogeneous spatial distribution of complex-shaped filler particles and spatial-gradient materials.

A necessary condition for the possibility of calculating temperature profiles in heterogeneous systems of complex geometry, along with using the concept of effective thermal conductivity, is the numerical calculation of the distribution of local heat fluxes (LHF).

Our work is devoted to the construction of maps of local heat fluxes of two-component composites both for single inclusions and for an array of inclusions with variable distribution characteristics in the matrix. In this work, we will investigate such a characteristic of the direction of local heat fluxes as the dependence of the weighted average angle of deviation on the relative concentration of inclusions. The study of the integral characteristics of two-component composite in this work was limited to the analysis of approximation formulas for the dependence of the effective thermal conductivity on the relative concentration.

2. Materials and methods

In this work, for numerical experiments, we used a quasi-two-dimensional model of a composite material (CM), i.e. a model in which heat transport was carried out only along two coordinates, and there was no heat transfer along the third coordinate. For this model, we numerically solved the Fourier differential heat conduction equation with boundary conditions of the first kind, namely, with fixed temperatures at the outer boundaries of the computational domain. In the absence of heat sources or sinks in the CM volume, the Fourier equation has the form

$$\nabla[\lambda(x, y), \nabla T(x, y)] = 0, \qquad (1)$$

where $T(x, y)$ is the temperature field and $\lambda(x, y)$ is the thermal conductivity. The value $\lambda(x, y)$, depending on the x and y coordinates, can be equal to the thermal conductivity of the matrix material (λ_m) or the thermal conductivity of the filler material (λ_f).

The model used a square shape for both filler particles (inclusions) and the matrix, which made it possible to use the finite difference method on an orthogonal grid with a step h in both coordinates to solve equation (1). The features of the calculation algorithm are described in detail in our previous works [9, 10]. As a result of solving equation (1), the temperature field and the field of vectors of the heat flux density were calculated according to the following equation

$$f(x, y) = -\lambda(x, y)\nabla T(x, y) \qquad (2)$$

In the course of numerical experiments, we simulated local heat fluxes both with the placement of heat-conducting inclusions in the matrix, and with exactly the same placement of heat-insulating inclusions in the matrix, and compared the simulation results in these two cases. The ratio of thermal conductivity of CM components λ_f / λ_m was chosen for the case of heat-conducting inclusions

approximately equal to the ratio of thermal conductivity of reinforcing steel and cement-sand stone (50 : 1), and for the case of heat-insulating inclusions equal to the ratio of thermal conductivity of expanded polystyrene and cement-sand stone (1 : 21).

The distribution of inclusions in the matrix was random and equiprobable. Both the matrix and the inclusions were square. The algorithm for creating the CM model made it possible to set the size of the matrix equal to a', the size of the inclusion equal to b' and the minimum allowable distance between the inclusions equal to d'. The indicated dimensions were expressed in whole numbers of steps of the computational grid h. The concentration of inclusions with was determined as the ratio of the total area occupied by the inclusions to the area of the matrix $c = N_f (b'/a')^2$, where N_f is the number of inclusions that was specified in the simulation. In CM model, unless otherwise specified, the side of the square of the matrix was chosen to be $128h$. When analyzing the results of numerical experiments, we operated on the following quantities: the relative size of the inclusions $b = b'/a'$ and the relative minimum distance $d = d'/b'$.

3. Results and discussion

As we have shown in [10], visualization of the density and LHF directions in CM models helps to correctly interpret the results of numerical experiments. Figures 1 – 4 show typical fragments of the calculated LHF maps in CM model with heat-insulating and heat-conducting inclusions. The degree of blackening of the map background is inversely proportional to the density of the LHF vector. Arrows show the direction of the vectors. In the area of the lowest-intensity LHF, to contrast with the dark background, the color of the arrows was changed to white. The temperature difference on all maps was applied from left to right.

Figure 1 shows the LHF map in the vicinity of a solitary heat-insulating inclusion of size $b = 0.125$. Figure 2 presents the LHF map in the vicinity of a solitary heat-conducting inclusion of equal size.
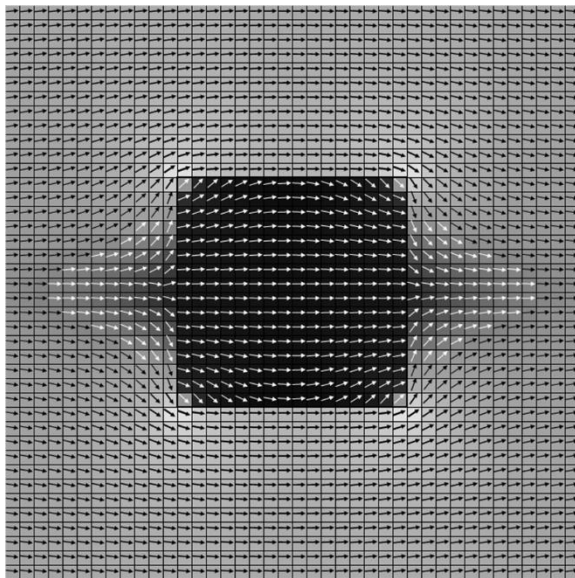
Figure 1. LHF map in the vicinity of heat-insulating inclusion.
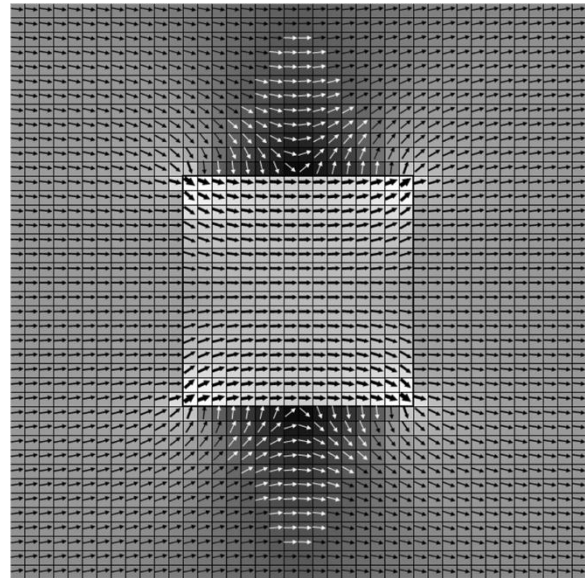
**Figure 2**. LHF map in the vicinity of solitary heat-conducting inclusion.

Figure 1 shows that LHF pass around the heat-insulating inclusion, forming regions with a low flux density (the so-called dark matrix) in the front and rear parts of the matrix, and regions with increased flux density along the upper and lower sides of the inclusion. In the case of a heat-conducting inclusion, as shown in figure 2, LHF from nearby regions of the matrix are concentrated inside the inclusion, with a dark matrix being formed along the upper and lower sides of the inclusion. The distortion of the LHF

direction in the vicinity of inclusion in both cases is recorded at a distance of the order of its size. Thus, if two inclusions of size b' are at a distance exceeding $2b'$, they can be considered as non-interacting. The maximum concentration of non-interacting inclusions in the two-dimensional case with a uniform distribution of inclusions over the matrix will be $1/9 \approx 0.11$. The nearest environment of each inclusion for the case of higher concentrations will affect the density and direction of the LHF in its vicinity.

Figure 3 shows a fragment of the LHF map in a matrix with interacting heat-insulating inclusions of size $b = 0.078$. Figure 4 presents a fragment of the LHF map in a matrix with exactly the same arrangement of heat-conducting inclusions.
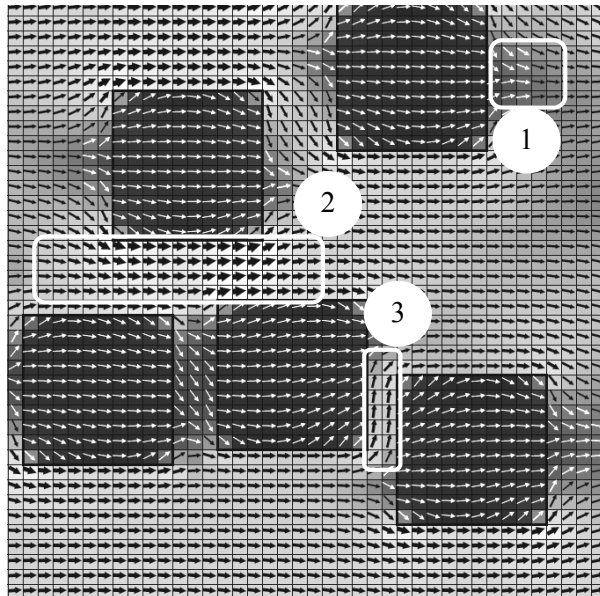
Figure 3. Fragment of the LHF map in the model with heat-insulating inclusions. Legend: 1 – dark matrix area; 2, 3 – regions of induced heat-conducting channels. Gray scale of LHF density: min ▭ max.
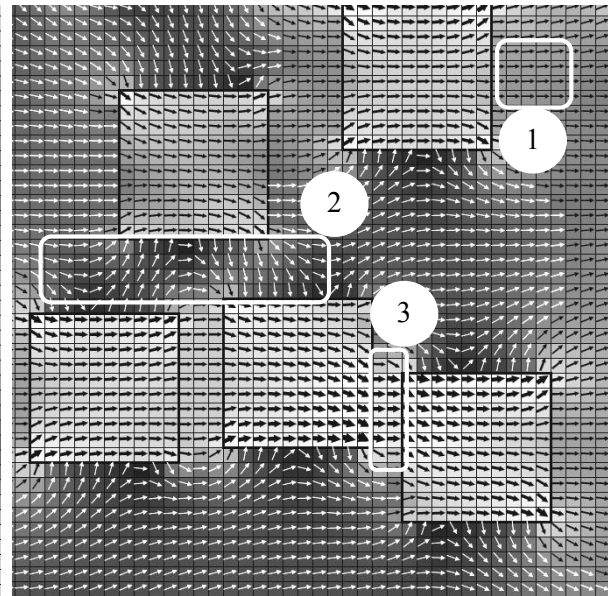
Figure 4. Fragment of the LHF map in the model with heat-conducting inclusions. The same areas are highlighted as in figure 3. Legend: 1 – unperturbed matrix area; 2 – dark matrix area; 3 – region of the induced heat-conducting channels.

Analysis of figure 3 shows that local heat fluxes tend to bend around heat-insulating inclusions and move along the matrix between them. The interaction of heat-insulating inclusions, as we have shown in [12], leads to the formation of extended induced heat-conducting channels, i.e. fragments of the matrix, through which the bulk of heat transfer is carried out. These channels have a sinuous shape, i.e. their length exceeds the distance between the hot and cold faces of the sample, and the local heat flux in these channels is directed at a certain angle with respect to the direction from the hot to cold faces.

In the case of heat-conducting inclusions (figure 4), local heat fluxes tend to concentrate in inclusions, and they overcome the heat-insulating matrix with a sufficient concentration of inclusions, migrating from inclusion to inclusion. Thus, also in this case, the local heat flux turns out to be directed at a certain angle with respect to the direction from the hot to the cold face.

Figures 5 and 6 show an example of the distribution of the local heat fluxes density with the same placement of inclusions of size $b = 0.039$ and concentration $c = 0.244$ with a minimum distance $d = 0.2$. The light color indicates the CM areas along which the bulk of heat transfer occurs (for a given set of CM parameters, this fraction is about 70%).

Figure 5 shows that in this case, the induced heat-conducting channels are formed between parallel chains of heat-insulating inclusions, while in Figure 6 it can be seen that the induced heat-conducting channels are formed by chains of closely spaced heat-conducting inclusions. In both cases, the direction

of the induced heat-conducting channels does not always coincide with the direction from the hot to the cold side; therefore, the path of the heat flow from the left to the right side will be greater than the distance between the sides, which leads to an effective increase in the thermal resistance of the material.
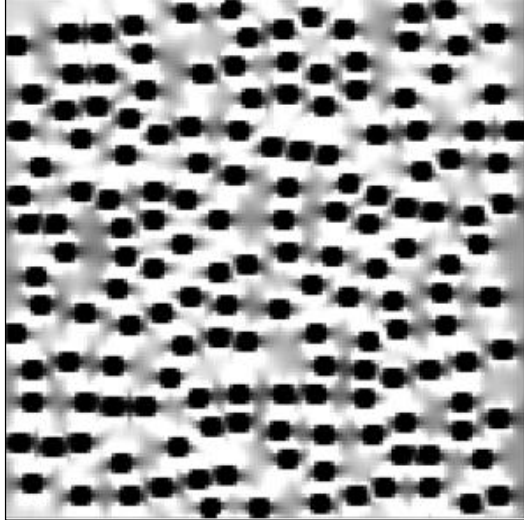
Figure 5. Density map of LHF in CM with heat-insulating inclusions.
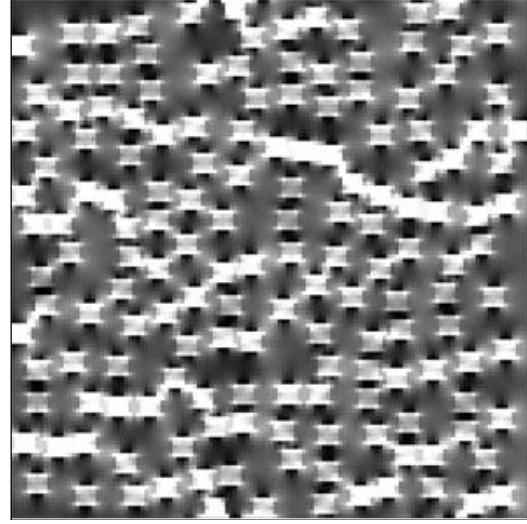
Figure 6. Density map of LHF in CM with heat-conducting inclusions.

Gray scale of LHF density: min ▬▬▬▭ max.

In order to describe the effective increase in the thermal resistance of the material, we introduced in [10] the value of the weighted average angle (WAA) of deviation of the direction of the local heat flux from the direction of the temperature difference on the sample faces

$$< \varphi_W >= \left(\sum_{i,j} \varphi_{i,j} \left| f_{i,j} \right| \right) \cdot \left(\sum_{i,j} \left| f_{i,j} \right| \right)^{-1} , \quad (3)$$

where $\left| f_{i,j} \right|$ is the modulus of the LHF density vector, calculated at the node of the computational grid with numbers i and j; $\varphi_{i,j}$ is the angle between the direction of the LHF vector and the direction of the temperature drop on the faces of the samples at the same node of the computational grid.

Numerical simulation allowed us to confirm that the weighted average angle $<\varphi_W>$ has a significant correlation with the effective thermal conductivity of the sample [10].

Figure 7 shows the dependence of $<\varphi_W>$ on the concentration of the filler for heat-insulating and heat-conducting inclusions of various sizes. The placement of heat-conducting inclusions in the CM leads to an increase in the angles of LHF deviation from the direction of the temperature drop at the edges of the samples as compared to the placement of heat-insulating inclusions. The monotonic growth of $<\varphi_W>(c)$ in the case of a heat-insulating filler is due to the fact that with an increase in the filler concentration, LHF are forced to bend around more obstacles. In this case, the path of the LHF increases. This should lead to a sublinear decrease in the effective thermal conductivity of CM λ_e. For a heat-conducting filler, the $<\varphi_W>(c)$ dependence has a sharp maximum, which shifts to the right with an increase in the size of the inclusions. In this case, LHF migrate from inclusion to inclusion, and $<\varphi_W>$ reflects the probable relative position of the inclusions. An initial growth in $<\varphi_W>$ with an increase in filler concentration is due to the fact that the number of inclusions available for migration of LHF, located at significant angles to the direction of the temperature drop, increases. Because in this case $\lambda_f / \lambda_m \gg 1$, then even with the lengthening of the total path of LHF, the thermal resistance along this path decreases. When a certain concentration is reached, the probability of finding an inclusion located

in the direction of the temperature difference increases, and as a result $<\varphi_W>$ decreases. Thus, it is natural to expect super linear growth of λ_e.
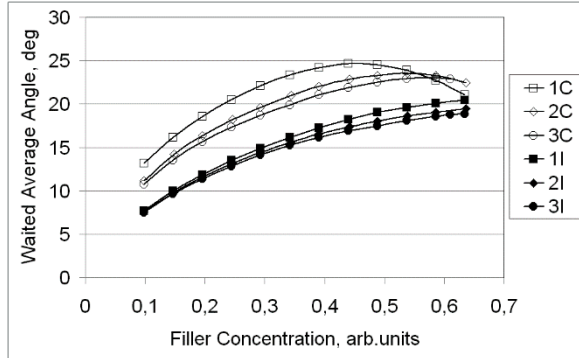
Figure 7. Dependences of $<\varphi_W>$ on the filler concentration. Filler dimensions: $1 - b = 0.039$; $2 - b = 0.0625$; $3 - b = 0.078$. Symbol «C» – heat-conducting inclusions; Symbol «I» – heat-insulating inclusions. For all dependencies: $d = 0$.
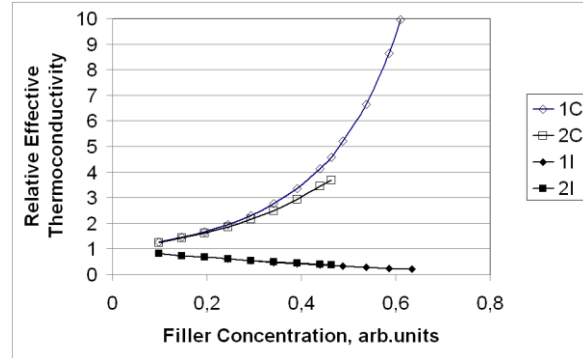
Figure 8. Dependences of λ_e / λ_m on the filler concentration. Minimum distance between filler particles: $1 - d = 0$; $2 - d = 0.2$. Symbol «C» – heat-conducting inclusions; Symbol «I» – heat-insulating inclusions. For all dependencies: $b = 0.078$.

Figure 8 shows the dependences of the relative effective thermal conductivity of CM λ_e / λ_m on the filler concentration for heat-insulating and heat-conducting inclusions with a size of $b = 0.078$ at two minimum distances d. In previous works [9, 10] we proposed an approximation of the dependence λ_e / λ_m on c for the case of a heat-insulating filler in the form

$$\frac{\lambda_e}{\lambda_m} = 1 - \frac{\alpha c}{\sqrt{(1+\beta c)^3}} ,\tag{4}$$

where α and β are fitting parameters. In the case of a heat-conducting filler, approximation (4) turns out to be inapplicable. Taking into account our new results, we propose to consider the approximation for the dependences of λ_e / λ_m on c in the form

$$\frac{\lambda_e}{\lambda_m} = \alpha + (1-\alpha)^{(1-c)} \left[\beta \left(\frac{\lambda_f}{\lambda_m} - \alpha \right) \right]^c ,\tag{5}$$

where α and β are also fitting parameters. In this case, for the heat-insulating filler ($\lambda_f / \lambda_m << 1$) the sign of the parameter α will be negative, and for the heat-conducting filler ($\lambda_f / \lambda_m >> 1$) the sign of the parameter α will be positive. The approximation parameters α, β and the coefficient of determination R^2 for the curves in figure 8 are given in table 1.

Table 1. Fit parameters and goodness of fit.

	Heat-insulating inclusions		Heat-conducting inclusions	
	$b = 0.078$; $d = 0$	$b = 0.078$; $d = 0.2$	$b = 0.078$; $d = 0$	$b = 0.078$; $d = 0.2$
α	-0.3000	-0.0111	0.7088	0,4284
β	0.8412	2.247	1.671	0.5007
R^2	0.9999	0.9996	0.9993	0.9998

4. Conclusions

1. With significant differences in the thermal conductivity of inclusions located in the composite matrix, and the thermal conductivity of the matrix itself, induced heat-conducting channels are formed in the composite material. The major part of heat transfer through the composite occurs through these channels. The ratio of the thermal conductivity of the inclusions and the matrix decisively affects the location of the induced heat-conducting channels and the direction of local heat fluxes. 2. The weighted average angle of deviation of the heat flux from the direction of the temperature difference between the faces of the samples is considered as an integral characteristic of the local heat fluxes direction. The explanation of the peculiarities of the dependences $<\varphi_W>$ on the filler concentration can be carried out using probabilistic ideas about the position of neighboring inclusions. 3. We have obtained a general formula for approximating the dependence of the effective thermal conductivity of the composite on the filler concentration for the cases of heat-insulating and heat-conducting inclusions. 4. The dependences $<\varphi_W>$ and λ_e / λ_m on the filler concentration are due to the peculiarities of heat transfer in composites at the micro level. The results obtained in this work can be used both for modeling the properties of composite materials and for optimizing technological processes for the manufacture of composites with specified thermophysical properties.

References

[1]   Agraval A, Satapathy A 2015 Mathematical model for evaluating effective thermal conductivity of polymer composites with hybrid fillers *Int. J. Therm. Sci* **89** 203-209
[2]   Angle J-P, Wang Z, Dames C and Mecartney M-L 2013 Comparison of two-phase thermal conductivity models with experiments on dilute ceramic composites *J. Am. Ceram. Soc* **96(9)** 2935-2942
[3]   Cao C, Yu A and Qin Q-H 2012 Evaluation of Effective Thermal Conductivity of Fiber-Reinforced Composites *Int. J. Archit. Eng. Constr* **1(1)** 14-29
[4]   Khan K-A, Khan S-Z and Khan M-A 2016 Effective thermal conductivity of two-phase composites containing highly conductive inclusions. *J. Reinf. Plast. Compos* **35(21)** 1586-1599
[5]   Ngo I-L, Byon C 2015 A generalized correlation for predicting the thermal conductivity of composite materials *Int. J. Heat Mass Tran* **83** 408-415
[6]   Duan H-L, Karihaloo B-L, Wang J and Yi X 2006 Effective conductivities of heterogeneous media containing multiple inclusions with various spatial distributions. *Phys. Rev B* **73(17)** 174203-13
[7]   Böhm H-J, Nogales S 2008 Mori–Tanaka models for the thermal conductivity of composites with interfacial resistance and particle size distributions *Compos. Sci. Technol* **68(5)** 1181-1187
[8]   Yin H-M, Paulino G-H, Buttlar W-G and Sun L-Z 2005 Effective thermal conductivity of two-phase functionally graded particulate composites. *J. Appl. Phys* **98(6)** 063704
[9]   Zaginaylo I, Maksimeniuk Ya and Pysarenko A 2017 Two-dimensional numerical simulation study of the effective thermal conductivity statistics for binary composite materials *Int. J. Heat Technol* **35(2)** 364-370
[10]   Pysarenko A and Zaginaylo I 2019 Numerical Simulation of the Heat Conductivity of Randomly Inhomogeneous Two-Dimensional Composite Material *Hauppage, New York: Nova Science Publisher's, Inc*. 176
[11]   Zaginaylo I V, Maximenouk Ya A and Pisarenko A N 2016 Induced thermally conductive channel influence on the formation of the insulating properties of binary composite materials *Construction, material science, mechanical engineering* ed V I Bolshakov (Dnipro) **92** 56-61